



Communication

Enhanced Photoelectrochemical Water Splitting of In_2S_3 Photoanodes by Surface Modulation with 2D MoS_2 Nanosheets

Roshani Awanthika Jayarathna ^{1,2,†} , Jun-Ho Heo ^{1,†} and Eui-Tae Kim ^{1,*}

¹ Department of Materials Science & Engineering, Chungnam National University, Daejeon 34134, Republic of Korea; rajayara@tec.rjt.ac.lk (R.A.J.); ppi6140@cnu.ac.kr (J.-H.H.)

² Department of Materials Technology, Faculty of Technology, Rajarata University of Sri Lanka, Mihintale 50300, Sri Lanka

* Correspondence: etkim@cnu.ac.kr

† These authors contributed equally to this work.

Abstract: Photoanodes with ample visible-light absorption and efficient photogenerated charge carrier dynamics expedite the actualization of high-efficiency photoelectrochemical water splitting (PEC-WS). Herein, we fabricated the heterojunction nanostructures of $\text{In}_2\text{S}_3/\text{MoS}_2$ on indium-doped tin oxide glass substrates by indium sputtering and sulfurization, followed by the metal–organic chemical vapor deposition of 2D MoS_2 nanosheets (NSs). The photocurrent density of $\text{In}_2\text{S}_3/\text{MoS}_2$ was substantially enhanced and higher than those of pristine In_2S_3 and MoS_2 NSs. This improvement is due to the MoS_2 NSs extending the visible-light absorption range and the type-II heterojunction enhancing the separation and transfer of photogenerated electron–hole pairs. This work offers a promising avenue toward the development of an efficient photoanode for solar-driven PEC-WS.

Keywords: photoelectrochemistry; water splitting; photoanodes; indium sulfide; molybdenum disulfide



Citation: Jayarathna, R.A.; Heo, J.-H.; Kim, E.-T. Enhanced Photoelectrochemical Water Splitting of In_2S_3 Photoanodes by Surface Modulation with 2D MoS_2 Nanosheets. *Nanomaterials* **2024**, *14*, 1628. <https://doi.org/10.3390/nano14201628>

Academic Editor: Andrey Chuvilin

Received: 14 September 2024

Revised: 4 October 2024

Accepted: 9 October 2024

Published: 11 October 2024



Copyright: © 2024 by the authors. Licensee MDPI, Basel, Switzerland. This article is an open access article distributed under the terms and conditions of the Creative Commons Attribution (CC BY) license (<https://creativecommons.org/licenses/by/4.0/>).

1. Introduction

Photoelectrochemical water splitting (PEC-WS) is propitious to produce hydrogen (H_2) to satisfy the world's energy demands and environmental challenges since H_2 gained its importance as an ideal carbon-free energy carrier and an alternative to fossil fuels in addition to its key roles in hydrogenation, petroleum refineries, and fertilizers [1,2]. However, the slow anode oxygen evolution reaction (OER) impedes the applicability of PEC-WS on a large scale [1]. As a solution, semiconductor photoanodes have gained research attention and become popular in solar energy conversion.

In_2S_3 , an n-type semiconductor, has attracted considerable attention due to its relatively narrow band gap of 2.0–2.3 eV for visible-light utilization, high photosensitivity, and chemical stability [3,4]. However, pristine In_2S_3 shows a relatively low PEC efficiency owing to its fast charge recombination inside the bulk and on the surface. Li et al. [5] reported $\beta\text{-In}_2\text{S}_3$ nanosheets (NSs) with a photocurrent density of $35.7 \mu\text{A}/\text{cm}^2$. Yao et al. [6] showed a PEC performance around $15 \mu\text{A}/\text{cm}^2$ by In_2S_3 NSs arrays. The formation of a heterojunction with an appropriate semiconductor can effectively minimize this drawback, resulting in improved charge separation and transfer and enhanced optical absorption.

Among the semiconductors that form favorable energy band alignments with In_2S_3 , 2D-layered MoS_2 can be a promising candidate because of its tunable bandgap energy, excellent photoexcitation, good chemical stability, and earth abundance [7,8]. It also exhibits tunable bandgaps from ~ 1.2 eV for the indirect gap of the bulk form to ~ 1.9 eV for the direct gap of the monolayer and a relatively high mobility (a few hundred cm^2/Vs) [8–10]. The photoelectrochemical (PEC) activity of 2D MoS_2 is also strongly affected by its architecture standing vertically on the substrate, which provides additional conductive channels for photoexcited carriers [11].

Information on the PEC-WS of In_2S_3 heterojunctioned with vertically-standing 2D MoS_2 NSs is limited. Singh et al. [12] reported the photocatalytic reaction of In_2S_3 functionalized with MoS_2 nanoflowers. Liu et al. [13] showed that MoS_2 nanodot-decorated In_2S_3 nanoplates can be applied for PEC but at a low photocurrent level of $1 \mu\text{A cm}^{-2}$. Sun et al. [14] later successfully applied a one-pot strategy for growing $\text{In}_2\text{S}_3/\text{MoS}_2$ with an anodic photocurrent of 0.06 mA cm^{-2} at 0.341 V vs. RHE ; nevertheless, the performance still has room for improvement. In the present study, we report vertical 2D MoS_2 NSs on In_2S_3 nanoparticles (NPs) as an alternative anodic choice to OER for significantly improved PEC-WS. The heterojunction effect of $\text{In}_2\text{S}_3/\text{MoS}_2$ was demonstrated through systematic PEC analysis and photo-excited carrier transfer properties across $\text{In}_2\text{S}_3/\text{MoS}_2$.

2. Materials and Methods

In_2S_3 was synthesized on indium-doped tin oxide (ITO) glass substrates via sputtering at 30 W power under a pressure of 3 mTorr for 40 s, followed by sulfurization under a H_2S flow rate of 200 standard cubic centimeters per minute (SCCM) at 300°C for 30 min under a pressure of 10 Torr. MoS_2 NSs were then decorated on the $\text{In}_2\text{S}_3/\text{ITO}$ and bare ITO substrates at 300°C for 8 min under a pressure of 1 Torr by using a metal-organic chemical vapor deposition (MOCVD) system with $\text{Mo}(\text{CO})_6$ and H_2S gas (5 vol. % in balance N_2) as Mo and S precursors, respectively. $\text{Mo}(\text{CO})_6$ was vaporized at 20°C and delivered into a quartz tube using Ar gas of 20 SCCM. The flow rate of H_2S gas was 65 SCCM.

The morphology of the samples was characterized via scanning electron microscopy (SEM, Hitachi S-4800). Their crystal structures were investigated by micro-Raman spectroscopy using an excitation band of 532 nm and a charge coupled device detector. Their optical property was characterized by UV-visible (UV-Vis) spectroscopy (Shimadzu UV-2600). PEC cells were fabricated on $1 \times 2 \text{ cm}^2$ ITO glass substrates. PEC characterization was performed using a three-electrode system with a Pt wire mesh as the working electrode and Ag/AgCl as the reference electrode. The electrolyte solution comprised $0.3 \text{ M KH}_2\text{PO}_4$ with KOH . The light source was a 150 W Xe arc lamp that delivers 100 mW/cm^2 simulated AM 1.5 G irradiation. PEC measurements, including linear sweep voltammograms (LSVs) recorded using a sourcemeter (Keithley 2400), and electrochemical impedance spectroscopy (EIS) were conducted using an electrochemical analyzer (potentiostat/galvanostat 263A) in a three-electrode reactor. EIS analysis was performed at a bias of 0.6 V while varying the ac frequency from 100 kHz to 100 mHz. The IPCE of the electrode structure was measured using a grating monochromator within the excitation wavelength range of 300–800 nm. The hydrogen gas products were analyzed using a YL 6500 gas chromatograph (Young In Chromass, Republic of Korea) equipped with a flame ionization detector and a thermal conductivity detector.

3. Results

Figure 1a–c exhibit the top- and tilted-view SEM images of In_2S_3 , 2D MoS_2 , and $\text{In}_2\text{S}_3/\text{MoS}_2$. In_2S_3 possessed a layer of NPs on the ITO substrate with the thickness of $\sim 50 \text{ nm}$ (Figure 1a). This particle network resembled a uniform structure that acted as a seed layer for MoS_2 growth. Vertically standing MoS_2 NSs were uniformly generated on the ITO substrate (Figure 1b) and In_2S_3 (Figure 1c). The morphological characteristics of MoS_2 on the entire surface of In_2S_3 appeared as vertically aligned NSs with a height of $\sim 180 \text{ nm}$ that developed by controlling the concentration ratio of Mo^{4+} to S^{2-} during the MOCVD reaction [11]. The adequate S^{2-} environment encouraged the growth of vertically-standing MoS_2 NSs on In_2S_3 .

The crystal structures of the samples (pristine In_2S_3 , pristine MoS_2 , and $\text{In}_2\text{S}_3/\text{MoS}_2$) were investigated by Raman spectroscopy. Our previous study revealed that the MoS_2 NSs are few-layer 2D structures [2,11], which was also confirmed by Raman spectra (Figure 1d). In_2S_3 exhibited Raman peaks around 255 and 297 cm^{-1} , corresponding to $\beta\text{-In}_2\text{S}_3$ [15], and two typical peaks of 2D-layered MoS_2 , corresponding to E^1_{2g} and A^1_{1g} modes [16] for the

in-plane vibration of S and Mo atoms and the out-of-plane vibration of S atoms, respectively. This finding indicates the successful growth of MoS₂ NSs on In₂S₃.

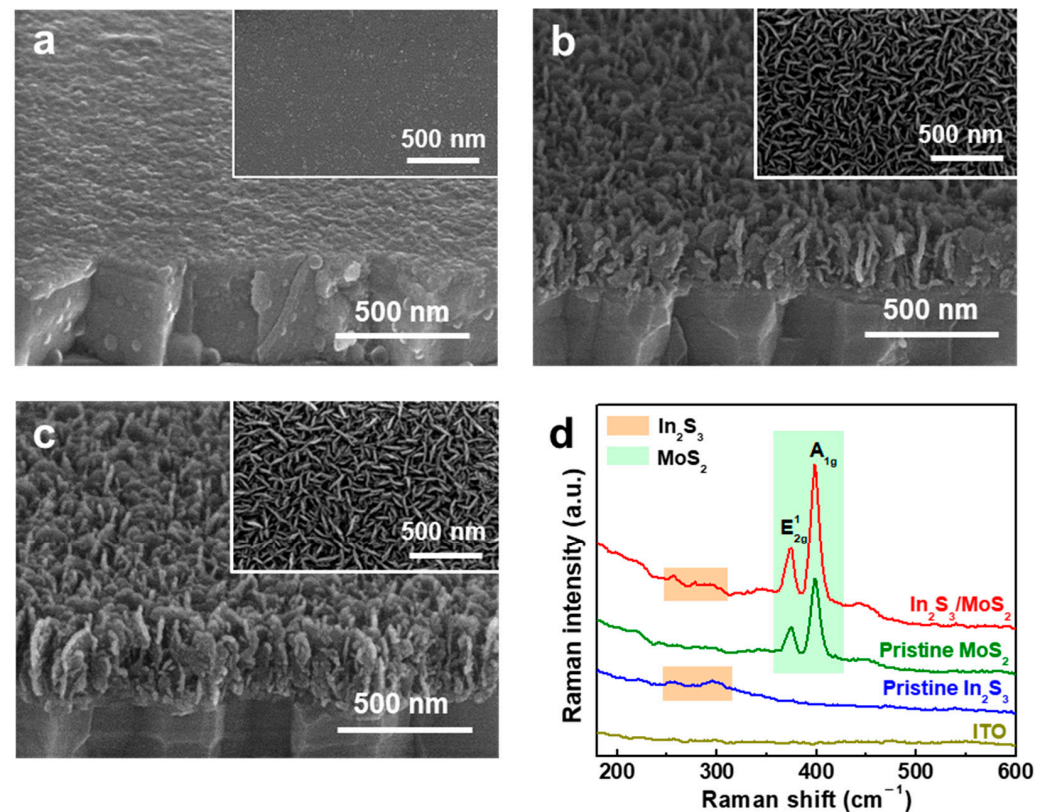


Figure 1. SEM images of (a) pristine In₂S₃, (b) pristine MoS₂, and (c) In₂S₃/MoS₂ and (d) Raman spectra of all films.

The optical properties evaluated by the UV–Vis absorbance analyses were strongly influenced by the presence of 2D MoS₂ as shown in Figure 2a. Pristine MoS₂ NSs exhibited an absorption edge of ~750 nm and two prominent absorption peaks at ~610 and ~665 nm, known as B and A excitons, respectively, which are correlated with direct excitonic transitions at the K point of the Brillouin zone [17]. Compared with pristine In₂S₃, the In₂S₃/MoS₂ heterostructure showed improved absorbance attributed to the enhanced surface scattering of MoS₂ 2D morphology. This result suggests a substantial improvement in the light absorption of the heterostructure with the decoration of MoS₂ NSs. The optical bandgap energies (Figure 2b) calculated according to the Tauc equation [18] were 2.12 eV (In₂S₃), 1.77 eV (MoS₂), and 1.78 eV (In₂S₃/MoS₂) as estimated from the intercept of the linear portion of the Tauc plot. The similar bandgaps of MoS₂ and In₂S₃/MoS₂ amplified the ability of MoS₂ for light absorption.

The PEC performance was evaluated by LSVs under simulation with AM 1.5 G illumination as depicted in Figure 3a. Compared with dark current curves, all the samples exhibited photocurrent attributed to the PEC reaction. The photocurrent density of pristine In₂S₃ was 0.097 mA/cm², and that of In₂S₃ heterojunctioned with MoS₂ was significantly improved up to 1.28 mA/cm² at 1.23 V vs. RHE, which was higher than that of pristine MoS₂ (0.85 mA/cm² at 0.93 V vs. RHE). The enhanced PEC properties can be attributed to the effective electron–hole separation and transfer through the heterojunction.

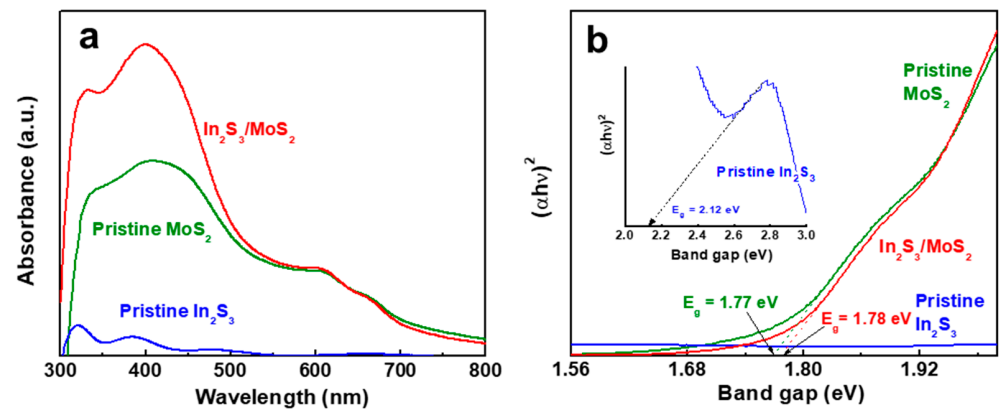


Figure 2. (a) UV-Vis absorption spectra and (b) Tauc plots of pristine In_2S_3 , pristine MoS_2 , and $\text{In}_2\text{S}_3/\text{MoS}_2$.

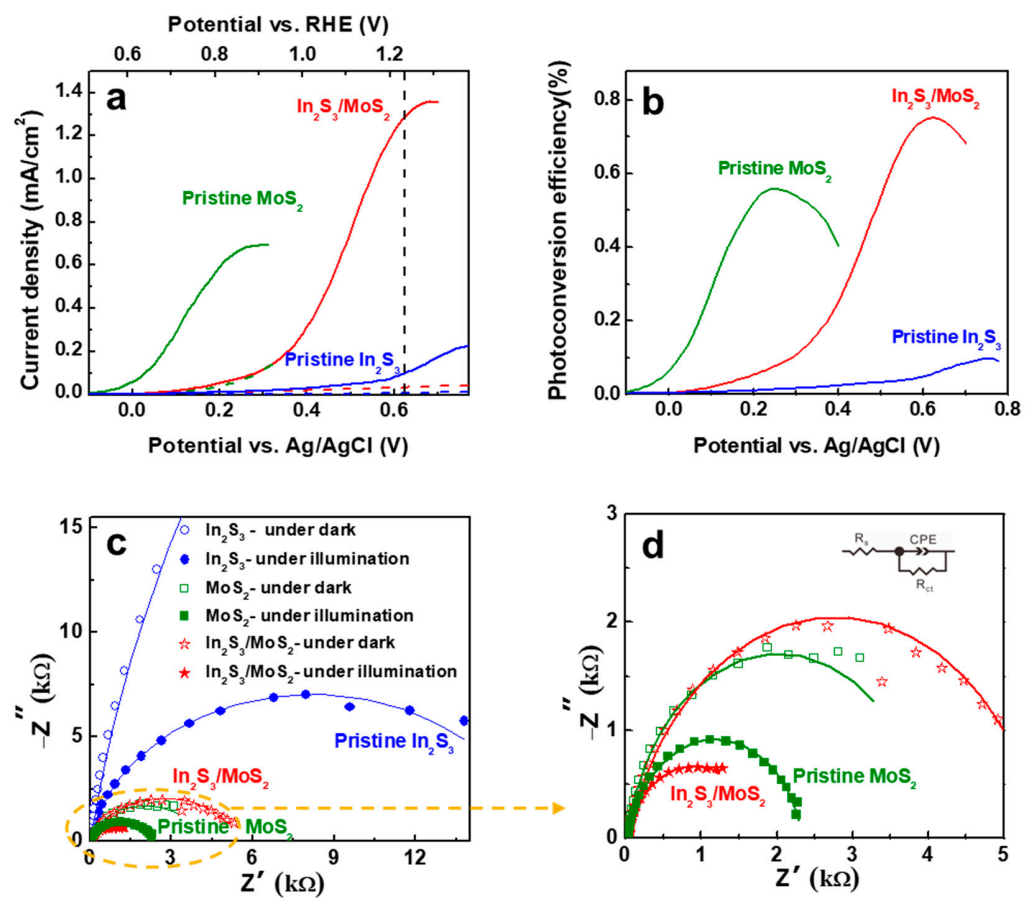


Figure 3. (a) Photo and dark current density–potential curves; (b) Photoconversion efficiency; and (c) Nyquist plots of PEC cells with pristine In_2S_3 , pristine MoS_2 , and $\text{In}_2\text{S}_3/\text{MoS}_2$. The yellow circle is enlarged in (d).

Figure 3b shows the photoconversion efficiencies (η) of the samples estimated using the following equation [19]:

$$\eta = J(E_0 - V_{\text{app}})/P_{\text{light}}$$

where J is the photocurrent density (mA/cm^2) at the applied potential, E_0 is the standard reversible potential (1.23 V), V_{app} is the applied potential, and P_{light} is the power density of illumination.

$\text{In}_2\text{S}_3/\text{MoS}_2$ showed an η of 0.75% at 1.23 V vs. RHE which was substantially higher than that of pristine In_2S_3 (~0.1%). Figure 3c,d show the Nyquist plots of the EIS fitted

using a simplified Randles circuit (inset in Figure 3d). $\text{In}_2\text{S}_3/\text{MoS}_2$ exhibited smaller EIS semicircles, indicating a lower charge transfer resistance (R_{ct}) of 1727Ω under illumination than the pristine samples ($16,350 \Omega$ and 2308Ω for In_2S_3 and MoS_2 , respectively). This result suggests that the heterojunction significantly improved the charge transfer efficiency.

A thorough study was performed using IPCE and H_2 evolution to understand how the heterojunction enhanced the PEC performance. $\text{In}_2\text{S}_3/\text{MoS}_2$ exhibited a peak value at $\sim 440 \text{ nm}$ and significant IPCE enhancement in the $600\text{--}750 \text{ nm}$ region (Figure 4a), which was affected by the surface modulation with 2D MoS_2 NSs. Hydrogen evolution from the dark cathode (Pt) was measured at 0.5 V versus Ag/AgCl using a three-electrode configuration for 30 min. The amount of produced H_2 was significantly increased by the $\text{In}_2\text{S}_3/\text{MoS}_2$ heterojunction as shown in Figure 4b, suggesting that the photocurrent was attributed to the WS. $\text{In}_2\text{S}_3/\text{MoS}_2$ formed a staggered heterojunction (Figure 4c) [2,20], which was effective in separating and subsequently transferring photogenerated electrons and holes to the cathode (Pt electrode) through In_2S_3 and onto the anode (MoS_2), leading to a boosted PEC performance.

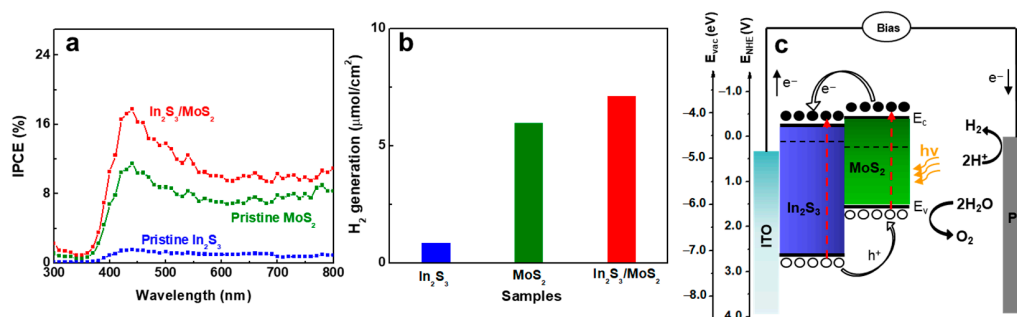


Figure 4. (a) IPCE plots and (b) hydrogen evolution amounts for 30 min of PEC cells with various working electrodes (pristine In_2S_3 , pristine MoS_2 , and $\text{In}_2\text{S}_3/\text{MoS}_2$) in $0.3 \text{ M KH}_2\text{PO}_4$ in KOH solution. (c) Schematic of the charge generation and transfer in the $\text{In}_2\text{S}_3/\text{MoS}_2$ PEC cell.

Figure 5a shows the photocurrent density–time (J - t) curves of all of the photoanodes over 30 min. The photocurrent of $\text{In}_2\text{S}_3/\text{MoS}_2$ stabilized after an initial decay period of $\sim 400 \text{ s}$, which was similar to that of pristine MoS_2 . The initial photocurrent decay was attributed to recombination of the photogenerated holes with electrons [11]. After PEC reaction, the peak positions of Raman and UV–Vis absorption spectra of $\text{In}_2\text{S}_3/\text{MoS}_2$ did not change, indicating no significant structural change. However, the full width at half maximum of Raman peaks slightly increased after reaction. Our recent study showed that MoS_2 NSs are susceptible to subtle morphological changes due to the decomposition of MoS_2 , mainly the loss of S elements during PEC reaction [11].

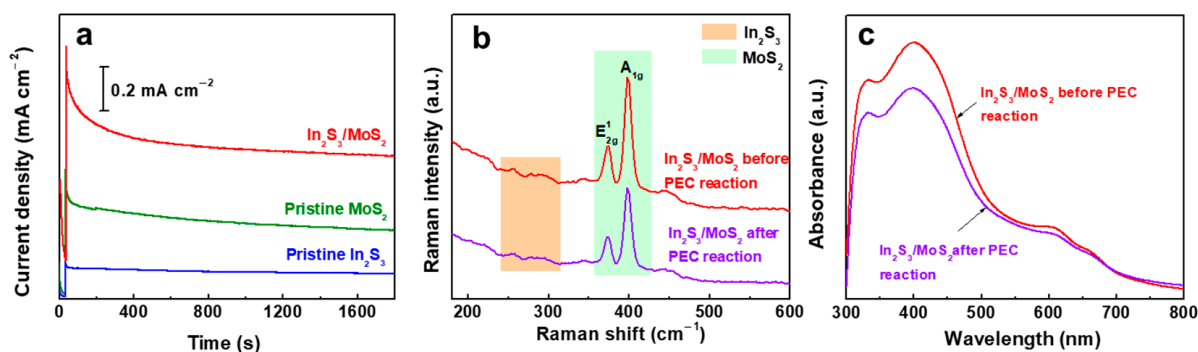


Figure 5. (a) Photocurrent–time plots for pristine In_2S_3 , pristine MoS_2 , and $\text{In}_2\text{S}_3/\text{MoS}_2$, and (b) Raman spectra and (c) UV–Vis absorption spectra of $\text{In}_2\text{S}_3/\text{MoS}_2$ before and after PEC reaction.

4. Conclusions

In this study, 2D MoS₂ NSs were vertically grown on a layer of In₂S₃ NPs using MOCVD. In₂S₃/MoS₂ exhibited up to more than 13 times and 1.5 times higher photocurrent densities than pristine In₂S₃ and pristine MoS₂, respectively, because of the extended visible-light absorption range and the efficient separation and transportation of the photogenerated carriers by the type-II heterojunction. The formation of a heterojunction with MoS₂ NSs led to the maximum photoconversion efficiency of In₂S₃/MoS₂ up to 0.75% at 1.23 V vs. RHE. This work suggests that the In₂S₃/MoS₂ heterojunction is one of the feasible photoanodes for efficient PEC-WS.

Author Contributions: Conceptualization, E.-T.K.; Methodology, R.A.J. and J.-H.H.; Data curation, R.A.J. and J.-H.H.; Formal analysis, R.A.J. and E.-T.K.; Software, R.A.J.; Visualization, R.A.J.; Writing—Original draft: R.A.J.; Writing—Review and Editing: E.-T.K. Supervision, E.-T.K. All authors have read and agreed to the published version of the manuscript.

Funding: This work was supported by Chungnam National University.

Data Availability Statement: Data are available in the main text.

Conflicts of Interest: The authors declare no conflicts of interest.

References

1. Jacobsson, T.J. Photoelectrochemical water splitting: An idea heading towards obsolescence. *Energy Environ. Sci.* **2018**, *11*, 1977–1979. [[CrossRef](#)]
2. Seo, D.-B.; Trung, T.N.; Kim, D.-O.; Duc, D.V.; Hong, S.; Sohn, Y.; Jeong, J.-R.; Kim, E.-T. Plasmonic Ag-decorated few-layer MoS₂ nanosheets vertically grown on graphene for efficient photoelectrochemical water splitting. *Nano-Micro Lett.* **2020**, *12*, 172. [[CrossRef](#)] [[PubMed](#)]
3. Horani, F.; Lifshitz, E. Unraveling the growth mechanism forming stable γ -In₂S₃ and β -In₂S₃ colloidal nanoplatelets. *Chem. Mater.* **2019**, *31*, 1784–1793. [[CrossRef](#)]
4. Lee, B.R.; Jang, H.W. β -In₂S₃ as water splitting photoanodes: Promise and challenges. *Electron. Mater. Lett.* **2021**, *17*, 119–135. [[CrossRef](#)]
5. Li, M.; Tu, X.; Su, Y.; Lu, J.; Hu, J.; Cai, B.; Zhou, Z.; Yang, Z.; Zhang, Y. Controlled growth of vertically aligned ultrathin In₂S₃ nanosheet arrays for photoelectrochemical water splitting. *Nanoscale* **2018**, *10*, 1153–1161. [[CrossRef](#)] [[PubMed](#)]
6. Yao, Y.; Wu, J.; Lv, B.; Wei, J.; Huang, R.; Wang, X.; Wang, W. NiO nanodot decorated In₂S₃ nanosheet arrays photoanode toward low-onset-potential photoelectrochemical hydrogen evolution. *Sol. Energy* **2024**, *273*, 112547. [[CrossRef](#)]
7. Ding, Q.; Song, B.; Xu, P.; Jin, S. Efficient electrocatalytic and photoelectrochemical hydrogen generation using MoS₂ and related compounds. *Chem* **2016**, *1*, 699–726. [[CrossRef](#)]
8. Frey, G.L.; Elani, S.; Homyonfer, M.; Feldman, Y.; Tenne, R. Optical-absorption spectra of inorganic fullerene like MS₂ (M = Mo, W). *Phys. Rev. B* **1998**, *57*, 6666. [[CrossRef](#)]
9. Li, H.; Zhang, Q.; Yap, C.C.R.; Tay, B.K.; Edwin, T.H.T.; Olivier, A.; Baillargeat, D. From bulk to monolayer MoS₂: Evolution of raman scattering. *Adv. Funct. Mater.* **2012**, *22*, 1385. [[CrossRef](#)]
10. Mak, K.F.; Lee, C.; Hone, J.; Shan, J.; Heinz, T.F. Atomically thin MoS₂: A new direct-gap semiconductor. *Phys. Rev. Lett.* **2010**, *105*, 136805. [[CrossRef](#)] [[PubMed](#)]
11. Trung, T.N.; Seo, D.B.; Quang, N.D.; Kim, D.; Kim, E.T. Enhanced photoelectrochemical activity in the heterostructure of vertically aligned few-layer MoS₂ flakes on ZnO. *Electrochim. Acta* **2018**, *260*, 150–156. [[CrossRef](#)]
12. Singh, J.; Soni, R.K. Enhanced sunlight driven photocatalytic activity of In₂S₃ nanosheets functionalized MoS₂ nanoflowers heterostructures. *Sci. Rep.* **2021**, *11*, 15352. [[CrossRef](#)] [[PubMed](#)]
13. Liu, F.; Jiang, Y.; Yang, J.; Hao, M.; Tong, Z.; Jianga, L.; Wu, Z. MoS₂ nanodot decorated In₂S₃ nanoplates: A novel heterojunction with enhanced photoelectrochemical performance. *Chem. Commun.* **2016**, *52*, 1867–1870. [[CrossRef](#)] [[PubMed](#)]
14. Sun, B.; Shan, F.; Jiang, X.; Ji, J.; Wang, F. One-pot synthesis of MoS₂/In₂S₃ ultrathin nanoflakes with mesh-shaped structure on indium tin oxide as photocathode for enhanced photo- and electrochemical hydrogen evolution reaction. *Appl. Surf. Sci.* **2018**, *435*, 822–831. [[CrossRef](#)]
15. Timoumi, A.; Belhadj, W.; Alamri, S.N.; Turkestani, M.K.A. Experimental studies and new theoretical modeling on the properties of In₂S₃ thin films. *Opt. Mater.* **2021**, *118*, 111238. [[CrossRef](#)]
16. Lee, C.; Yan, H.; Brus, L.E.; Heinz, T.F.; Hone, J.; Ryu, S. Anomalous lattice vibrations of single and few-layer MoS₂. *ACS Nano* **2010**, *4*, 2695–2700. [[CrossRef](#)] [[PubMed](#)]
17. Eda, G.; Yamaguchi, H.; Voiry, D.; Fujita, T.; Chen, M.; Chhowalla, M. Photoluminescence from chemically exfoliated MoS₂. *Nano Lett.* **2011**, *11*, 5111–5116. [[CrossRef](#)] [[PubMed](#)]

18. Dai, J.; Zhu, Y.; Tahini, H.A.; Lin, Q.; Chen, Y.; Guan, D.; Zhou, C.; Hu, Z.; Lin, H.-J.; Chan, T.-S.; et al. Single-phase perovskite oxide with super-exchange induced atomic-scale synergistic active centers enables ultrafast hydrogen evolution. *Nat. Commun.* **2020**, *11*, 5657. [[CrossRef](#)] [[PubMed](#)]
19. Khan, S.U.M.; Al-Shahry, M.; Ingler, W.B., Jr. Efficient photochemical water splitting by a chemically modified n-TiO₂. *Science* **2002**, *297*, 2243–2245. [[CrossRef](#)] [[PubMed](#)]
20. Bernède, J.C.; Barreau, N.; Marsillac, S.; Assmann, L. Band alignment at β -In₂S₃/TCO interface. *Appl. Surf. Sci.* **2002**, *195*, 222–228. [[CrossRef](#)]

Disclaimer/Publisher’s Note: The statements, opinions and data contained in all publications are solely those of the individual author(s) and contributor(s) and not of MDPI and/or the editor(s). MDPI and/or the editor(s) disclaim responsibility for any injury to people or property resulting from any ideas, methods, instructions or products referred to in the content.